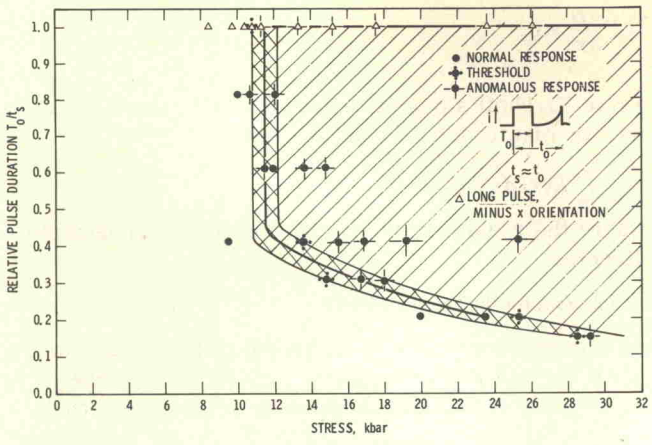

FIG. 4. Experiments at various stresses result in either a normal response or an anomalous response. The location of each experiment is shown with an indication of whether the response of the gauge is normal or anomalous. The region in which anomalous response is observed is indicated by the shaded region. The cross-hatched region indicates the area where either normal or anomalous response is observed. When the threshold conditions are grossly exceeded, larger anomalous currents are observed. For comparative purposes, experiments on $-x$-orientation long-duration loading are shown along the line $T_0/t_s = 1.0$. Data include experiments from the present work and from Ref. 9. The anomaly is not observed for $+x$ orientation long-duration loading.

played graphically in Fig. 4. The symbolism used for each experimental point in the figure indicates whether normal response or anomalous response was observed. As a secondary symbolism, the length of the lines surrounding each point indicates the extent of the anomaly; longer lines represent larger anomalies. Several experiments were conducted in the immediate vicinity of the thresholds where the current-time trace indicated only a very slight anomaly. The input-stress threshold for anomalous response is fit to the data with a cross-hatched band to indicate the zone where different values were obtained in the various experiments. The scatter in threshold values is believed to result from the variable acmite speck concentrations among the various samples. Each inclusion tends to act as a point of stress and electric field concentrations.

The threshold for anomalous response is found to have distinctly different characteristics depending upon the relative pulse duration. For relative pulse durations greater than $0.45t_s$, the anomaly is independent of relative pulse duration and is observed to occur whenever a stress of 11.2 ± 0.7 kbar is exceeded. Experiments on $-x$ orientation samples with long-pulse loading show the same threshold stress value, indicating a connection between the two phenomena.

For pulse durations less than $0.45t_s$, the threshold is found to be strongly dependent upon the pulse duration. In fact, the data indicate that with pulse durations less than $0.1t_s$, normal response will be observed at stresses as high as 40 kbar. In any event, stress pulses with durations less than $0.45t_s$ seem to exhibit an entirely different character from that of the longer duration pulses, indicating that different physical mechanisms control the anomalous response in the two pulse duration ranges. It should be emphasized that until unloading occurs, the gauges experience exactly the same conditions as in the previous long-pulse loading experiments and the gauge response is normal in all respects.

C. Residual Current Observations

After unloading and before the anomalous currents were observed, all experiments indicated a "residual" current of +1% of the maximum value. The small residual current may be a consequence of the small difference between Hugoniot loading wave velocity and adiabatic unloading wave velocity under conditions in which the polarization is not a linear function of stress. Furthermore, a tendency for the residual current to drift slightly downward late in time [see Fig. 3(a)] indicates that the one-dimensional character of the geometry is slightly perturbed very late in time.

In order to interpret the experimental observations on a physical basis, it is necessary to develop an analysis describing the electric fields for short-duration pulse loading. The conductivity of quartz has previously been shown to depend strongly upon the amplitude of the electric field and upon the polarity of the field relative to the shock front. Thus, in Sec. IV, relations for the electric fields will be developed based upon an electrostatic analysis.

IV. ELECTROSTATIC ANALYSIS

The present analysis is similar to that previously developed[6,9] for x-cut quartz under step-function loading. It is assumed that the resistivity of the piezoelectric disk is infinite. This assumption will permit explicit determination of the electric fields immediately prior to any conductivity indicated in the experimental records. In particular, the analysis will give values of the electric fields at the conductivity thresholds described in Sec. III.

The electric fields in shock-loaded quartz are a direct consequence of the piezoelectric polarization. These electric fields are uniform throughout a region of uniform polarization; but, even though the polarization is uniform, the field intensities change in time to accomodate the equal-potential condition between the electrodes. The electric field intensities at a given time depend directly on the stress amplitudes with a typical value about 10^6 V/cm at 20 kbar. Although a field of this magnitude is less than that required for dc dielectric breakdown,[20] 6×10^6 V/cm, it is a source of concern, particularly because of the large mechanical stresses to which the disk is subjected. Fortunately, the field analysis is based on straightforward physical principles and assumptions which are readily tested in the shock-loading experiments. Assumptions used in the analysis do not introduce errors larger than 1%; the principal error in the field calculation is the magnitude of the piezoelectric polarization, which according to previous work is known to within ±2.5%.

A. Electrostatic Relations

The analysis is based upon the general premise that the shock propagation speed is very much less than the propagation speed of an electromagnetic wave. Thus

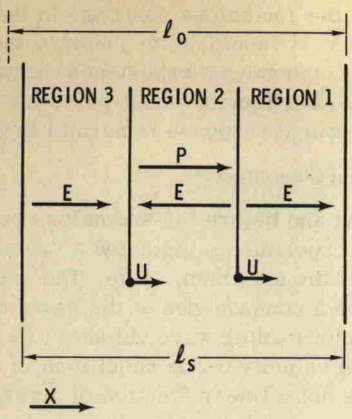

FIG. 5. Various electrical and mechanical regions along the thickness of the piezoelectric disk are shown for times when the short-duration pulse is entirely contained within the disk. Region 1, ahead of the front, is unstressed but experiences an electric field. The stress pulse in region 2 produces a region of uniform polarization proportional to the stress amplitude. Region 3, behind the unloading shock front, is unloaded to zero stress and zero polarization.

electrostatic relations are used to describe the electrical parameters, and the dynamical aspects are assumed to be controlled by the transient mechanical response. Although this situation seems reasonable, the analysis neglects an important "feedback" mechanism, electromechanical coupling, which operates to change the dynamical solution controlled by the shock propagation. This is a small (~1%) effect in quartz but can be as large as ~25% in ferroelectric materials.[21]

The problem will be restricted to the short-pulse loading problem presently being considered such that the geometric arrangement can be depicted as shown in Fig. 5. A section through the thickness of the disk, l_s, at some characteristic time after the pulse is contained within the disk shows three characteristic regions. Region 1 is the unstressed region ahead of the loading shock front; region 2 is the region of uniform stress and piezoelectric polarization with thickness UT_0; region 3 is the unstressed region behind the unloading shock front. Region 3 has been stressed to the input-stress value and subsequently reduced to zero stress. Since both the unloading and loading fronts have velocities, equal to a constant value U, region 3 has a thickness equal to $U(t-T_0)$.

The solution for the electric fields follows directly from three fundamental electrostatic relations. It is convenient to define an electric displacement D, which for our one-dimensional configuration is taken to be

$$D \equiv P + \epsilon E, \tag{4}$$

where P is the piezoelectric polarization, whose polarity is detected in compression with conventional electronic instruments, ϵ the permittivity, and E the electric field. If there is no free charge within the disk, i.e., the resistivity is infinite, Coulomb's law leads to Laplace's equation $\nabla^2\phi = 0$ which for one-dimensional conditions gives the result

$$\frac{\partial D}{\partial x} = 0. \tag{5}$$

From Kirchoff's law the external short circuit between the two electrodes is expressed as

$$\int_0^t E(x)\,dx = 0, \tag{6}$$

where the x axis is taken along the shock propagation direction.

B. Solutions for the Electric Fields

As a consequence of Eq. (5) the electric displacements in all regions are the same at a given time. Since $P_1 = P_3 = 0$, it follows immediately from Eq. (4) that $\epsilon_1 E_1 = \epsilon_3 E_3$. Assuming that $\epsilon_1 = \epsilon_3 = \epsilon_2 = \epsilon$, the unstressed permittivity,[22] it follows that $E_1 = E_3 \equiv E_{1,3}$. Thus regions 1 and 3 are identical from the electrical point of view and their thicknesses l_1 and l_3 change in time depending upon the wave speed.

The relation among the fields in the various regions is obtained from the short-circuit condition, Eq. (6), which shows that

$$E_2 l_2 + E_{1,3}(l_1 + l_3) = 0, \tag{7}$$

where l_2 equals $T_0 U$, and $l_1 + l_3 = l_s - T_0 U$. Applying Eqs. (4) and (5),

$$\epsilon E_1 = \epsilon E_3 = \epsilon E_{1,3} = P + \epsilon E_2. \tag{8}$$

Substituting the relation for E_2 from Eq. (7) into Eq. (8) gives the field in the unstressed regions:

$$E_{1,3} = \frac{+P}{\epsilon}\,\frac{T_0}{t_s}, \quad T_0 < t < t_0 \tag{9}$$

and in the stressed region

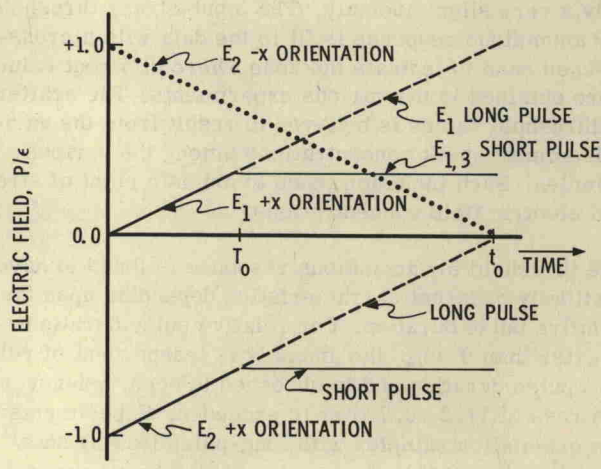

FIG. 6. Electric fields in the various regions are uniform at a given time. The field-amplitude—vs-time relations for the various regions are as indicated. Before stress unloading occurs, the fields are as indicated by the dotted line. After stress unloading occurs, the fields are constant in time and the amplitude of the field in the unloaded region is proportional to the relative pulse duration T_0/t_s. The polarity of the field in the unloaded region is such that electrons are accelerated away from a source located immediately behind the unloading wave front.